On the Lateral Instability of a Thin Beam under Periodic Bending Loads

Pak Chol-Hui*

(Received February 20, 1995)

The lateral instability of a thin beam under periodic bending loads was investigated. Physical evidences of the instability were observed previously by experiments. But an analytical study has not been reported. The object of this study is to demonstrate the nature and existence of dynamic lateral instability. The harmonic balance method is applied to bifurcation modes which result from the stability change of torsional mode of a beam and then compared with numerical simulations. It is found, in a certain frequency range, that a small bending load results in the lateral instability when damping is small.

Key Words: Dynamic Lateral Instability of Beams, Bifurcation Mode, Natural Forcing Function, Normal Modes, Generating Function

1. Introduction

The lateral instability of a thin beam under periodic bending loads is studied. The lateral instability under static loads is well known as the lateral buckling of beams (Timoshenko, 1934) and has been extensively investigated in elastic stability problems. The instabilities of simple structures under periodic loads have been studied by many investigators, e.g., see Bolotin (1964). Dynamic lateral instabilities of thin beams were observed by experiments (Cusumano and Moon, 1995, Part I; Kim, 1995), but an analytical investigation has not been reported. It was believed that the dynamic instability occurs due to a special mode in the free vibrations of thin beams. This mode is a coupled bending-torsional mode which is unusual in the sense that the beam may be bent in a large constant deflection accompanying torsional oscillations.

The coupled nonlinear equations are not available in order to describe motions of uniform elastic rods having general cross-sections which can be bent in two principal directions of cross-section and can be twisted at the same time. Cusumano and Moon (1995, Part II) derived the equations of motion for a thin elastica by assuming that the elastica can be bent only in the flexible direction. In this study, their equations of motion will be utilized.

It has later been found (Pak et al., 1992) that the unusual mode is the bifurcation mode resulting from the stability of torsional normal mode. A basic theory will be described to formulate series of procedures of computing the bifurcation mode and the forced responses associated with it. In order to show the dynamic lateral instability of thin beams, the basic theory will be applied. Since some assumptions were posed to develop the basic theory, computer simulations are performed to verify its validity. Then the results of theory are compared with those of numerical simulations.

2. Experimental Evidences

Cusumano (1995, Part I) performed an experimental study on the nonlinear dynamics of a flexible cantilevered steel rod having a thin cross-section ($0.21^{mm} \times 12.7^{mm}$) and a length 288^{mm}. The elastica was forced by sinusoidally displacing the clamped end in the flexible direction. In a certain set of system parameters, torsional displacements were observed, and the further increase in forcing

* Inha University

amplitude resulted in chaotic motions. The measurements by strain gages showed very unusual vibrations that the bending strains contained large constant values plus oscillating parts while the torsional strains oscillated with double the period of bending oscillations.

A similar experimental study was done by Kim (1995). A uniform cantilevered aluminum rod having a cross-section ($4^{mm} \times 20^{mm}$) and a length 910^{mm} was fixed vertically with the clamped end downward and then was forced by sinusoidally displacing the clamped end in the flexible direction. In a certain range of forcing frequency and forcing amplitude, coupled bending-bending vibrations were observed by measurement with accelerometers, as discussed by Nayfeh and Pai (1989). In other ranges of forcing frequency and forcing amplitude, coupled bending-torsional vibrations were observed by an optical device; a laser beam is projected on a mirror attached to the rod and the mirror reflects the laser beam on a vertical screen so that the bending motion of rod traces a vertical line, while the torsional motion a horizontal line on the screen. The coupled bending-torsional vibrations are observed as a closed curve. In some parameter ranges, the closed curves are ellipses flat in the horizontal direction, implying that the torsional displacement of rod becomes dominant under bending loads.

3. Basic Theory

3.1 Objective

We shall be interested in computing bifurcation modes that result from the stability change of an existing mode in nonlinear systems having certain symmetries, frequently observed in mechanical systems. In the systems considered here, the ratios of linear frequencies are not necessarily commensurable, e.g., not close to one−to−N, N=1, 2, 3, ... , internal resonance condition (Nayfeh, 1979). By utilizing the procedure of computing bifurcation modes, the associated forced responses can be calculated for weakly damped and forced systems. We are interested in formulating procedures to explicitly describe the view of Rosenberg (1966) that a nonlinear resonance occurs when the forcing frequency is close to nonlinear natural frequency. Here the resonance refers to a large steady state vibration under a small forcing amplitude.

3.2 System description and normal modes

Consider elastically and inertially coupled nonlinear conservative systems in which the kinetic energy T and potential energy V are expressed in the form

$$\begin{aligned} T &= \frac{1}{2}\sum_{i,j=1}^{2} m_{ij}(\boldsymbol{x})\,\dot{x}_i\dot{x}_j \\ V &= V(\boldsymbol{x}) \\ T + V &= h \end{aligned} \tag{1}$$

where $\boldsymbol{x} = (x_1, x_2)$ is the generalized coordinate vector, h the total energy, m_{ij} inertially coupling parameters, and dots represents differentiation with respect to time t. Assume that $V(x)$ is positive definite, and for a given h, the motions remain in a bounded region $h - V(x) \geq 0$ in the configuration space. And assume that $V(-x) = V(x)$ and $m_{ij}(-x) = m_{ij}(x)$.

When h is sufficiently small, the system is integrable and every motion remains on a two-dimensional invariant torus. As h becomes large, the torus is destroyed so that infinitely many periodic motions are created through series of bifurcations (Guckenheimer and Holmes, 1983; Ott, 1993). General procedures are not available to compute those periodic motions. There are, however, two special periodic motions, known as the normal modes. At a sufficiently small energy h, they are the linear normal modes and continuously extended to large systems energy. The existence of normal modes (Pak and Rosenberg, 1968), the bifurcations of normal modes (Johnson and Rand, 1979; Rand et al., 1992) and the stability behaviors of bifurcation modes (Pak, 1989) were reported. When the system energy h is very small, normal modes are stable since the linear normal modes are always stable. As h is increased, they may become unstable. If the stability change is plotted in Poincar map, an elliptic center is replaced by a saddle, as depicted in Fig. 1 (a) and (b).

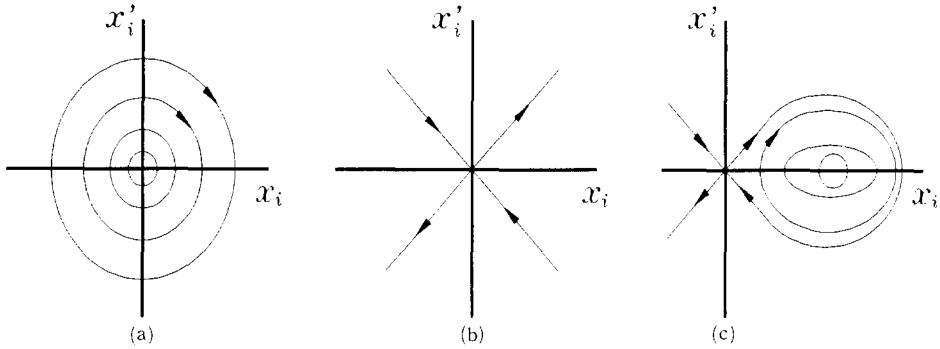

Fig. 1 Poincaré maps to show the stability change of a periodic motion in conservative Hamiltonian systems (a) stable motion (b) unstable motion (c) formation of saddle-loop

Further assume that the stable and unstable manifolds are connected to form a saddle-loop. Then there exists an elliptic center in the loop, creating a newly born periodic motion, called a bifurcation mode. It is clear that the bifurcation mode is born as elliptically stable. In general, the loop is formed in systems having symmetry, such as $m_{ij}(-x)=m_{ij}(x)$ and $V(-x)=V(x)$.

3.3 Stability analysis of periodic motion

In order to evaluate the stability of periodic motions, the equations of motion are written by Lagrange's formulation

$$\frac{d}{dt}\left\{\sum_j m_{ij}(\boldsymbol{x})\dot{x}_j\right\}-\frac{1}{2}\sum_{j,k}\frac{\partial m_{jk}(\boldsymbol{x})}{\partial x_i}\dot{x}_j\dot{x}_k+\frac{\partial V(\boldsymbol{x})}{\partial x_i}=0,\ i=1,2. \tag{2}$$

Then by perturbing the periodic motion of Eq. (2) and linearizing, we obtain a linear system of two coupled second order differential equations having periodic coefficients. Floquet theory may be applicable to evaluate the stability, but it is practically too difficult to compute four Floquet exponents. However, it is well known by the symplectic property (Ott, 1993; Meirovitch, 1970) that the sum of every pair of exponents vanishes. In particular, when the system is conservative, one pair of Floquet exponent vanishes identically and hence the remaining two exponents determine the stability of periodic motion; elliptically stable when they are imaginary, and hyperbolic (saddle) when real. To determine the non-identically vanishing exponents, a conservative Hamiltonian system having two degrees of freedom is transformed by Birkhoff (1927) into a forced Hamiltonian system of single degree of freedom, called reduced Hamiltonian system, through the action and angle formulation. But it is practically impossible to obtain the reduced system for the purpose of stability analysis.

Synge (1926) utilized the concept of Riemannian geometry to study the dynamics of Hamiltonian systems. The equation of motion is described by the calculus of variations. The trajectory passing through two configurations, P_1 and P_2, is the geodesic curve by Jacobi least action principle

$$\delta\int_{P_1}^{P_2}\sqrt{2(h-V(\boldsymbol{x}))}\,ds=0,$$
$$ds^2=\sum_{i,j=1}^{2}m_{ij}(\boldsymbol{x})\,dx_i dx_j \tag{3}$$

Then he defined the disturbance Vector $\vec{\beta}$ between the unperturbed trajectory C* and perturbed trajectory C, not by the condition of simultaneity (Lyapunov sense) but by the condition of orthogonality as shown in Fig. 2.

Then he derived the equation governing the magnitude β

$$\ddot{\beta}+Q(t)\beta+2x\delta h=0 \tag{4}$$

where $Q(t)=Kv^2+3\kappa^2v^2+\Sigma V_{ij}n_in_j$ evaluated along the unperturbed trajectory C*, k the curvature of C*, K the Gaussian curvature of metric of Eq. (2), v the velocity of C*, $V_{ij}=V_{ij}=\nabla\nabla V$, and δh an infinitesimal difference of h between C* and C. Then the stability of C* is defined; C* is

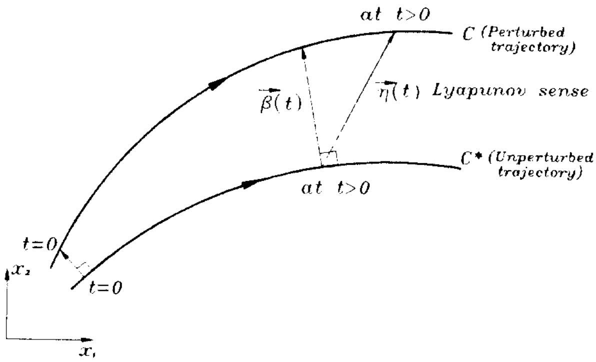

Fig. 2 The disturbance vector $\vec{\beta}(t)$

stable in the kinematico-statical sense if every solution of Eq. (4) is bounded. Since the stability of C^* can be evaluated at every fixed h, it is regarded that $\delta h=0$ in what follows. The coefficient $Q(t)$ is periodic because the unperturbed motion is periodic and Floquet theory is applicable. It is possible to write $Q(t)=\overline{Q}+\tilde{Q}(t)$ where $\overline{Q}$ is the mean value and $\tilde{Q}(t)$ the fluctuating part of $Q(t)$. Then Eq. (4) can be rewritten in the form

$$L\beta=-\overline{Q}\beta \tag{5}$$

where L is a linear operator given by

$$L=\frac{d^2}{dt^2}+\tilde{Q}\ (\mathrm{t}).$$

3.4 Computation of bifurcation modes

The stability chart consists of the boundary curves that separate the sets of system parameters in which the periodic motion is stable, called the stable regions, from the other sets in which the motion is unstable, called the unstable regions. In constructing the boundary curves, it is required to find a periodic solution of Eq. (5) having the period τ or 2τ, where τ is the period of $Q(t)$. Such periodic solutions are called the eigenfunctions and such values of $\overline{Q}$ the corresponding eigenvalues (McLachlan, 1964).

In order to compute the newly born bifurcation mode which is located in the saddle-loop as an elliptic center as shown in Fig. 1 (c), It is assumed that the eigenfunction of Eq. (5) is the seed of bifurcation mode (Pak et al., 1992). Let us denote $\vec{x}^*(t)$ and $\vec{\beta}^*(t)$ as the unperturbed periodic motion and the associated eigenfunction, respectively. At the bifurcation point, the perturbed motion $\vec{x}(t)$ is written as

$$\vec{x}(t)=\vec{x}^*(t)+\vec{\beta}^*(t) \tag{6a}$$

With the further increase in total energy, this equation can be assumed to be the generating function to describe the bifurcation mode. If this function is decomposed into each generalized coordinate in the form

$$x_i(\omega t)=x_i^*(\omega t)+\beta_i^*(\omega t),\quad i=1,2 \tag{6b}$$

and if the results are substituted into Eqs. (2), the harmonic balance method can be applicable.

3.5 Computation of forced responses

The stability chart associated with Eq. (5) is usually presented in a two-dimensional plane with one axis representing the total energy h or the amplitude of unperturbed periodic motion and with the other axis representing other systems parameters. Since the bifurcation mode is born as stable, as depicted from Fig. 1 (c) and remains stable within at least a small interval of h (Magnus and Winkler, 1966), there exists a nonempty stable region in the stability chart.

At first, we shall be interested in formulating procedures to compute the forced responses associated with the bifurcation mode in undamped systems. Choose an interior point P in the stable region of the stability chart. Let α (P) be the systems parameters corresponding to P, and $\vec{\beta}(t,\alpha)$ the eigenfunction of Eq. (5). Under small variations $\delta\alpha$ of systems parameters, the varied bifurcation mode remains in the stable region. Then we define a natural forcing function $\vec{f}(t)$ as

$$\vec{f}(t) = \Sigma C_i \frac{\partial \vec{\beta}(t,\ \alpha)}{\partial \alpha_i} \delta \alpha_i \qquad (7)$$

where, C_i is an arbitrarily chosen small constant, and $\delta\alpha_i$ variation of individual parameters. When this forcing function is applied to the system, the response will naturally be another bifurcation mode, slightly varied from the earlier mode. In a similar way, the concept of natural forcing function was designed in order for easiness of computing forced responses (Harvey, 1958; Vakakis, 1991).

The natural forcing function (7) forms a vector space of finite dimensions equal to the number of mutually independent systems parameters including h, implying a wide variety of choice. Since the eigenfunction $\vec{\beta}^*$ (t) of Eq. (5) is expressed in a series of infinite harmonics, the natural forcing function is not practical. However, the first few terms are dominant and an approximated forcing function may be used. When the approximate natural forcing function is applied, the system is no longer conservative, but becomes a time-dependent Hamiltonian. If the forced response is periodic, then it is elliptically stable since the bifurcation mode is elliptically stable, and the identically vanishing pair of Floquet exponents are shifted to the imaginary axis by a small amount, as shown in Fig. 3.

When small dampings are added to the system in addition to approximate natural forcing function, the forced response can be calculated by use of the harmonic balance method. It is expected that the Floquet exponents move to the left in the complex plane and the forced response becomes asymptotically stable.

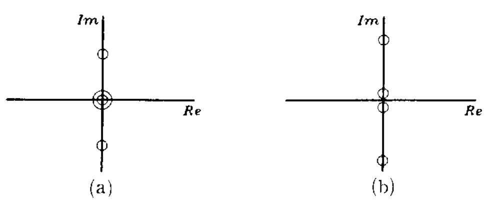

Fig. 3 Floquet exponents in case of (a) bifurcation mode of Fig. 1 (c) and (b) forced response under an approximate natural forcing function

3.6 Concluding remarks

The procedure formulated above, is applicable to strongly nonlinear systems in which usual perturbation techniques are rarely available. The formulation was described through heuristic approaches, not based on rigorously logical foundations. The assumptions, posed in the procedure, should be verified. In particular, the formulation of saddle-loop is important. If the saddle-loop is not formed, the stable and unstable manifolds of the saddle may intersect transversally implying, via the Smale-Birkhoff theorem (Guckenheimer and Holmes, 1983), that the invariant set contains a countable infinity of periodic unstable motions, an uncountable set of non-periodic motions and a dense orbit. Having verified the formation of saddle-loop, it should be demonstrated that the eigenfunction of Eq. (5) is a good candidate of generating functions to compute the bifurcation mode by the harmonic balance method. In practice, the natural forcing function is approximated by a single harmonic term. In this case, it should be verified that the forced response is periodic. In some systems, multiple forced responses are possible. Then the stability analysis should be performed on each forced response.

4. Equations of Motion for Thin Beams

Consider a uniform and straight elastic rod which can be bent and twisted. For small motions, the linear theory is applicable; the bending and torsion are decoupled so that solutions are obtained by superposition. However, when motions are not small, bending and torsion are coupled by the geometric nonlinearity due to the curvature and inertia effects. Modern rod theory, e.g., Crespo and Glynn (1978, Part I), is based on geometrically exact displacement configurations; planar cross-section remains plane. But when a rod having non-circular cross-section is twisted, the cross-section is warped. In this view, exact and explicitly written equations of motion are hardly obtained.

A rod having general cross-section can be bent in two principal axes of cross-section and can be twisted at the same time. The linear natural frequency of the first torsional mode is much greater than that of the first bending mode in the order of aspect ratio (the length of rod divided by the thickness). Therefore it is hardly expected to have the condition of internal resonance (Nayfeh, 1979) between bending and torsional modes. Crespo and Glynn (1978, Part II) derived the forced equations of motion, describing the coupling between two bending modes in the principal directions of cross-section. The torsional displacement is assumed to be coupled only elastically. In the resulting equations, the torsional degree of freedom is neglected. Utilizing these equations of motion, Pai and Nayfeh (1990) studied nonplanar bending vibrations of beams having rectangular cross-sections.

Cusumano and Moon (1995, Part I), through experimental studies on nonlinear dynamics of thin elastica, have found that the torsional degree of freedom is important. By assuming that the elastica is not bent in the stiff direction, the coupled bending-torsional equations of motion are derived. After proper simplifications and neglect of the nonlinear curvature effect, the derived kinetic energy T and potential energy V are written in dimensionless form

$$T=\frac{1}{2}\int_0^1[(\frac{\partial u}{\partial t})^2+(\mu+u^2)(\frac{\partial \phi}{\partial t})^2]ds$$
$$V=\frac{1}{2}\int_0^1[(\frac{\partial^2 u}{\partial s^2})^2+\frac{1}{(1+V)}(\frac{\partial \varphi}{\partial s})^2]ds \qquad (8a)$$

where u is the bending displacement, ϕ the torsional displacement, μ the inertial coupling parameter, ν Poisson ratio, and s spatial variable along the center line. Applying the cantilevered boundary conditions and truncating the equations in the first bending and the first torsional modes, the resulting kinetic and potential energies are obtained

$$T=\frac{1}{2}(1+\alpha y^2)\dot{x}^2+\frac{1}{2}\dot{y}^2$$
$$V=\frac{1}{2}(p^2x^2+y^2) \qquad (8b)$$

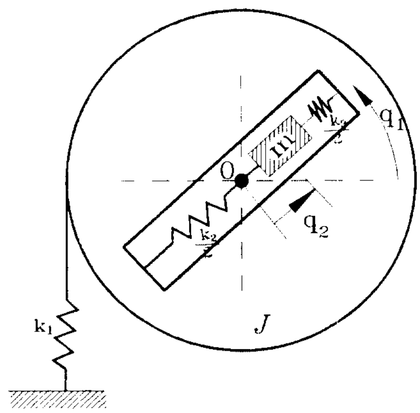

Fig. 4 A simple mechanical analogue to a thin elastica

where x is the torsional displacement, y the bending displacement divided by a characteristic length, α the coupling parameter, and p the frequency ratio (p=59 in their experiments). They showed that the system given by Eq. (8b) is equivalent to a discrete system shown in Fig. 4.

It is noted that for the thin elastica (thin beam in this paper) having boundary conditions other than cantilevered one, the resulting equations have the same form as Eq. (8b). The equations of motion are written as

$$(1+\alpha y^2)\ddot{x}+2\alpha y\dot{y}\dot{x}+p^2x=0$$
$$\ddot{y}-\alpha\dot{x}^2y+y=0. \qquad (9)$$

5. Bifurcation Mode of Thin Beams

It is readily seen from Eq. (11) that there are two special periodic motions. The motion having $y\equiv 0$ and $x\not\equiv 0$ is the torsional normal mode and the one having $x\equiv 0$ and $y\not\equiv 0$ is the bending normal mode. To determine the stability of torsional mode in which the motion is described by $x=A\ sin\ pt$ and $y=0$, the disturbance $\vec{\beta}=(0, \beta)$ is given to the y-direction only, according to Synge's concept described in section 3, the resulting equation is written

$$\frac{d^2\beta}{d\tau^2}+(\delta+2\varepsilon\cos 2\tau)\beta=0 \qquad (10a)$$

where

$$\delta=\frac{1}{p^2}-\frac{\alpha}{2}A^2,\ \varepsilon=-\frac{\alpha}{4}A^2,\ \tau=pt. \qquad (10b)$$

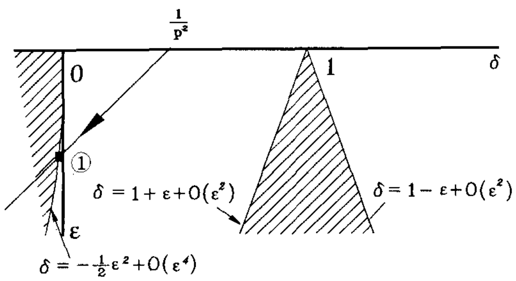

Fig. 5 Stability chart for the torsional mode (shaded areas mean unstable and the torsional mode becomes unstable at the point ①)

The stability of torsional mode is changed when the arrowed line crosses the boundary curve $\delta = -1/2\varepsilon^2 + O(\varepsilon^4)$, as shown in Fig. 5.

It is stable for small amplitude A and becomes unstable for large A ($A^2 > 2/\alpha p^2$ when $p \gg 1$). The eigenfunction corresponding to this boundary curve is written as

$$\vec{\beta}(t) = c\left(1 - \frac{1}{2}\varepsilon\cos 2pt + \frac{1}{32}\varepsilon^2\cos 4pt\right) + O(\varepsilon^3) \qquad (11)$$

where, $\vec{\beta}(t)$ is in the y-direction, and c an arbitrarily chosen small constant.

To show the formation of saddle-loop through the stability change of torsional mode, Poincaré map is plotted in Fig. 6.

It is noted that two saddle-loops are formed, representing a pitch-fork bifurcation, due to the symmetry of Hamiltonian $H(-q, -p) = H(q, p)$ in this system. Two elliptically stable bifurcation modes are born, called nonlocal mode (Pak et al., 1992). Utilizing the eigenfunction (11), the nonlocal mode can be computed by the concept of Eq. (6b). An approximate generating function is assumed for harmonic balance method;

$$x(t) = A\sin\omega t,$$
$$y(t) = B + C\cos 2\omega t. \qquad (12)$$

Substitute Eq. (12) into the Eqs. (9) of motion to obtain

$$B - \frac{1}{2}\alpha\omega^2 A^2\left(B + \frac{1}{2}C\right) = 0 \qquad (13a)$$

$$(1 - 4\omega^2)C - \frac{1}{2}\alpha A^2(B + C) = 0 \qquad (13b)$$

$$A\left[p^2 - \omega^2 - \alpha\omega^2\left(B^2 - BC + \frac{1}{2}C^2\right)\right] = 0 \qquad (13c)$$

From Eq. (13c), $A = 0$ is a solution. Then it is readily seen that $B = C = 0$, implying no motion. This case is excluded. Eliminate ω^2 and A^2 from Eqs. (13) to obtain

$$4p^2 C\left(B + \frac{1}{2}C\right) + \left(B^2 - \frac{1}{2}C^2\right) + \alpha\left(B^2 - \frac{1}{2}C^2\right)\cdot\left(B^2 + BC + \frac{1}{2}C^2\right) = 0.$$

Let us transform the variables B and C into the polar coordinates

$$B = R\cos\theta,\ C = R\sin\theta,\ s = \tan\theta \qquad (14)$$

to obtain

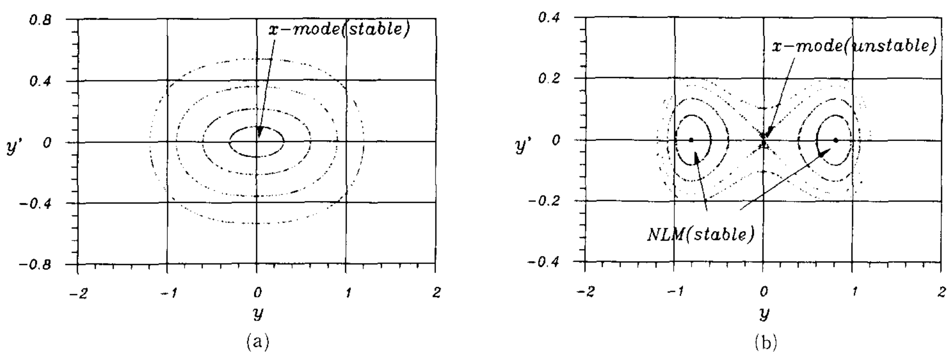

Fig. 6 Poincaré maps to show the formation of saddle-loop when the torsional mode changes its stability (a) stable torsional mode (b) unstabilized torsional mode and two other bifurcation modes (nonlocal modes) (System parameters used are $\alpha = 0.1$, $p = 20$, and $h = 15.0$)

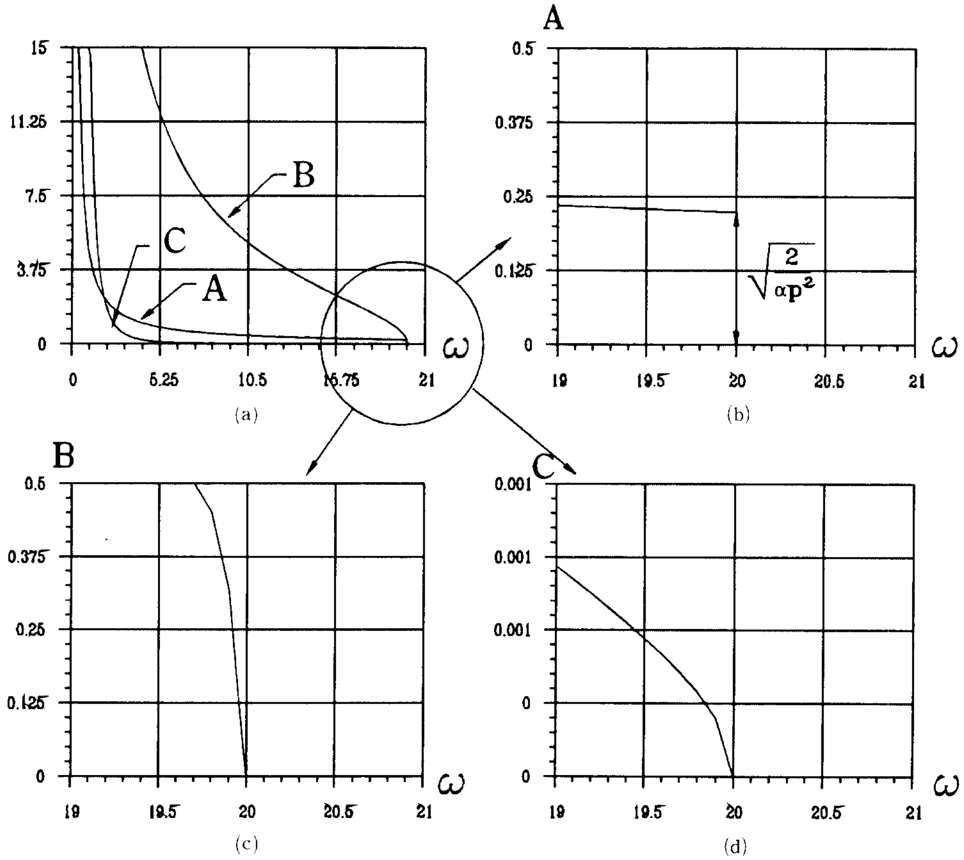

Fig. 7 Backbone curves of nonlocal mode ($\alpha=0.1$, $P=20$)

$$f(s)+\mu g(s)=0 \tag{15}$$

where

$$f(s)=(1+s^2)[(2p^2-\frac{1}{2})s^2+4p^2s+1]$$

$$g(s)=(1-\frac{1}{2}s^2)(\frac{1}{2}s^2+s+1)$$

$$\mu=\alpha R^2.$$

Then ω^2 and A^2 are recovered and written as

$$\alpha A^2=\frac{16s}{s^2-2},\ \omega^2=\frac{s^2-2}{4s(s+2)}. \tag{16}$$

The procedure of computing nonlocal mode is as follows ; given μ, first compute s from Eq. (15), then compute ω^2 and A^2 from Eq. (16), and B and C from Eq. (14). The graphs A (ω), B (ω), and C (ω) are called the backbone curves of nonlocal mode, as shown in Fig. 7 and the modal curves are computed numerically by Runge-Kutta algorithm and shown in Fig. 8.

The nonlocal mode has some special properties that they does not exist when $h<h_0$, h_0 is the energy at the bifurcation, they are born at the stability change of torsional mode, and they contain both constant bending displacement B and oscillating part C. As h increases through h_0, B becomes much greater than C, the frequency of oscillating part begins twice of torsional motion, and frequency-doubling process occurs at the further increase in h.

To compare the analytical results of nonlocal mode with numerical simulations, the modal curve is written in a geometrical form as shown in Fig. 9.

$$y=a_0+a_2x^2$$

where

$$a_0=B+C,\ a_2=-\frac{2B}{A^2},\ \text{and}\ a=a_0+a_2A^2.$$

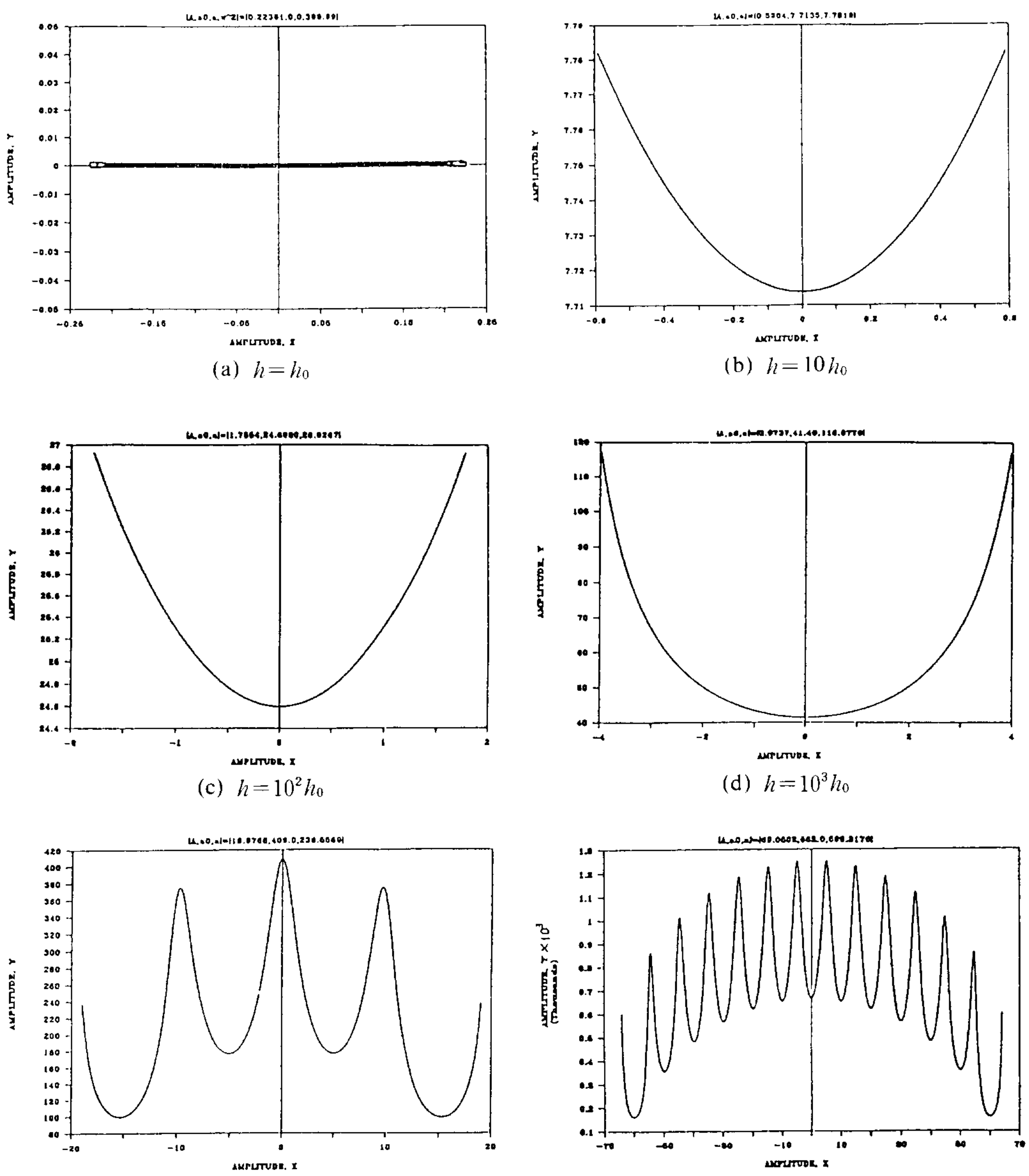

(a) $h=h_0$ (b) $h=10h_0$

(c) $h=10^2h_0$ (d) $h=10^3h_0$

(e) $h=10^4h_0$ (f) $h=10^5h_0$

Fig. 8 Modal curves of nonlocal mode (h_0 is the total energy at the bifurcation point. $a=0.1$, $p=20$, $h_0=10.0$)

Parameters A, a_0 and a, shown in Fig. 9, and natural frequency ω of nonlocal mode are calculated both by the theory given in Eqs. (12)~(14) and by Runge-Kutta are listed in Table. 1. From Fig. 9 and Table. 1, theory is agreeable with numerical simulation up to the total energy $h=10^3h_0$.

The nonlocal modes are born as elliptically stable, as depicted in Fig. 6. It is shown by Lee (1995) that, having computed the modal curve of nonlocal mode and utilized Singe's stability Eq. (5), the nonlocal mode is shown analytically to be born as elliptically stable.

The stability of bending mode ($x=0$, $y=Bcost$) can be analyzed in a similar way. The stability equation is derived

$$[1+\varepsilon(1+\cos 2t)]\frac{d^2\beta}{dt^2}$$
$$-2\varepsilon\sin 2t\frac{d\beta}{dt}+p^2\beta=0 \qquad (17)$$

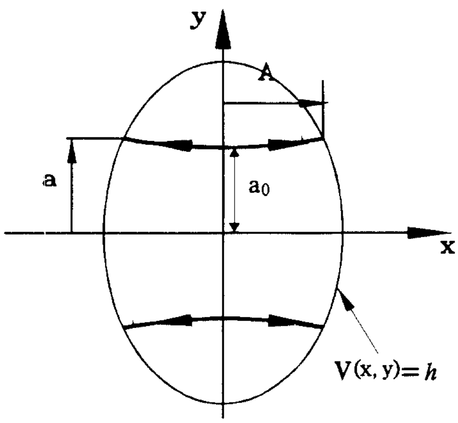

Fig. 9 Modal curve of the nonlocal mode

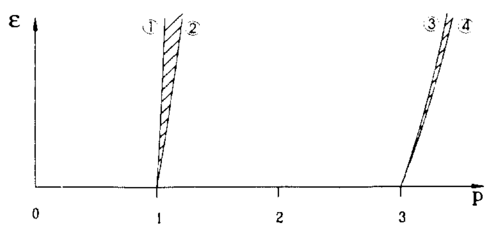

Fig. 10 Stability chart of the bending mode : curve ① $p^2=1+\varepsilon/2-9\varepsilon^2/32+O(\varepsilon^3)$, curve ② $p^2=1+3\varepsilon/2-9\varepsilon^2/32+O(\varepsilon^3)$, curve ③ $p^2=9(1+\varepsilon-23\varepsilon^2/32+185\varepsilon^3/512+O(\varepsilon^4))$, and curve ④ $p^2=9(1+\varepsilon-23\varepsilon^2/32+183\varepsilon^3/512+O(\varepsilon^4))$

where $\varepsilon={}^1/_2\alpha B^2$. The stability chart is constructed (Pak et al., 1992), as shown in Fig. 10.

It is noted that, for even p, two boundary curves coincide, a situation called "coexistence (Magnus and Winkler, 1966)" and hence the associated instability region disappears.

6. Forced Responses

When an undamped thin beam is excited by periodic bending load, the equations of motion are written

$$(1+ay^2)\ddot{x}+2ay\dot{y}x+\bar{p}^2x=0$$
$$\ddot{y}-a\dot{x}^2y+y=F_0\cos 2\omega t \qquad (18)$$

The forced responses can be computed by using properly chosen approximate natural forcing function as described in section 3. The natural forcing function is derived from the variations of eigenfunction $\vec{\beta}^*(t, \alpha)$ due to small variations of systems parameters. Therefore an approximate natural forcing function can be derived by the variations of generating function given by Eq. (12) and can be written in the form

$$F_x=\delta A\sin\omega t$$
$$F_y=\delta B+\delta C\cos 2\omega t \qquad (19)$$

where F_x and F_y are torsional and bending loads, respectively, δA, δB and δC are arbitrarily chosen small constants, representing forcing amplitudes. This arbitrariness implies that the right hand side of Eq. (18) is an approximate natural

Table 1 Comparisons of theory and numerical calculation (R-K) for nonlocal mode ($\alpha=0.1$, p=20, $h_0=10.0$ bifurcation value).

h		h_0	$10h_0$	$100h_0$	10^3h_0
A	Theory	0.2236	0.5907	1.7998	5.0412
	R-K	0.2236	0.5904	1.7854	3.9737
a_0	Theory	0.0000	7.7056	24.4740	53.038
	R-K	0.0000	7.7135	24.5980	41.400
a	Theory	0.0000	7.7731	26.5378	99.1701
	R-K	0.0000	7.7816	26.9267	116.9779
ω^2	Theory	400.000	57.4404	6.3015	0.9275
	R-K	399.998	57.3065	6.2118	1.2219

forcing function.

Assume the forced responses of the form of Eq. (12), and substitute into Eq. (18) to obtain

$$B-\frac{1}{2}\alpha A^2\omega^2(B+\frac{1}{2}C)=0 \quad (20a)$$

$$(1-4\omega^2)C-\frac{1}{2}\alpha A^2\omega^2(B+C)=F_0 \quad (20b)$$

$$A[p^2-\omega^2-\alpha\omega^2(B^2-BC+\frac{1}{2}C^2)]=0 \quad (20c)$$

From Eq. (20c), A=0 is a solution. Then it is found from Eq. (19a) that B=0, implying the pure bending response

$$y\ (t)=\frac{F_0}{(1-4\omega^2)}\cos 2\omega t$$

The stability of this response can be determined in a similar manner to the bending mode and be found that it is elliptically stable if ω is not near to p/ (2N), N=1, 3, 5, $\cdots$. When $A\neq 0$, it is possible from Eq. (20) to compute A, B and C as the solutions associated with nonlocal mode. The frequency responses are computed and shown in Fig. 11 for small F_0 and they are very near to the backbone curves. To show the periodicity and stability of forced response associated with nonlocal mode, Poicaré map and time histories are shown in Fig. 12.

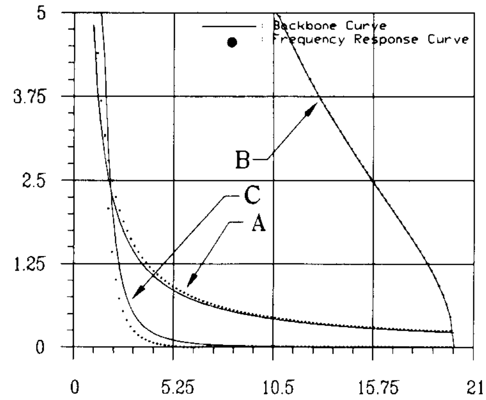

Fig. 11 Frequency response curves when $\alpha=0.1$, p=20, $F_0=1.0$ (The abscissa corresponds to frequency and the ordinate, to amplitudes.)

For damped and forced systems, the equations of motion are written

$$(1+\alpha y^2)\ddot{x}+2\alpha y\dot{y}\dot{x}+2p\zeta_1\dot{x}+p^2x=0$$
$$\ddot{y}-\alpha\dot{x}^2+2\zeta_2\dot{y}+y=F_0\cos 2\omega t \quad (21)$$

where ζ_1 and ζ_2 are modal damping factors. The solutions are assumed in the form

$$x(t)=A\sin(\omega t-\varphi_1)$$
$$y(t)=B+C\sin(2\omega t-\varphi_2) \quad (22)$$

Substitute Eqs. (22) into Eqs. (21) to obtain

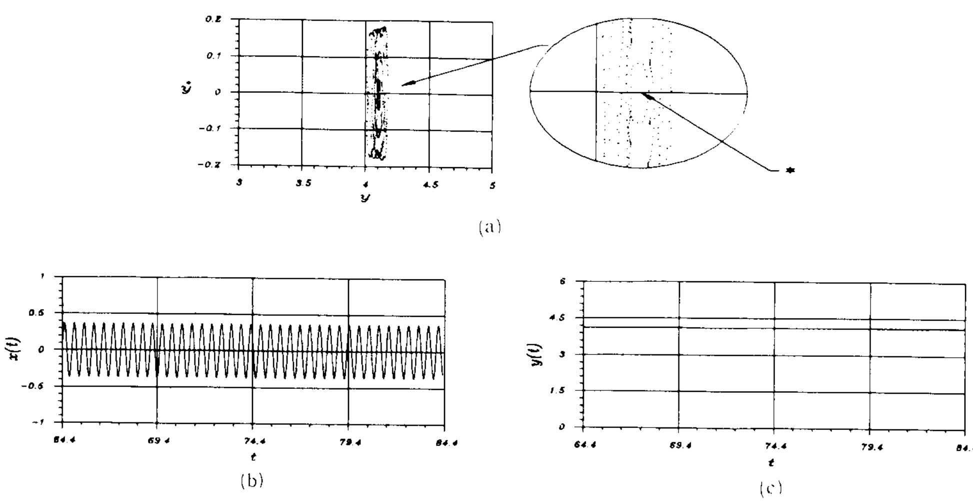

Fig. 12 (a) Poincoré map in the y-y′ plane (It is plotted for several initial conditions near that of nonlocal mode response and the symbol ′ * ′ locates nonlocal mode response.) and (b), (c) time responses of x (t) and y (t), respectively ($\alpha=0.1$, p=20, $\omega=12.2$, $F_0=1.0$)

$$A\left\{2p\zeta_1\omega\sin\varphi_1+[p^2-\omega^2-\alpha\omega^2(B^2+\frac{1}{2}C^2)]\cos\varphi_1-\alpha BC\omega^2\cos(\varphi_1-\varphi_2)\right\}=0$$

$$A\left\{2p\zeta_1\omega\cos\varphi_1-[p^2-\omega^2-\alpha\omega^2(B^2+\frac{1}{2}C^2)]\sin\varphi_1-\alpha BC\omega^2\sin(\varphi_1-\varphi_2)\right\}=0$$

$$B-\frac{1}{2}\alpha A^2\omega^2 B-\frac{1}{4}\alpha A^2 C\cos(2\varphi_1-\varphi_2)=0 \qquad (23)$$

$$\alpha A^2 B\omega^2\sin 2\varphi_1+C(1-4\omega^2-\frac{\alpha}{2}A^2\omega^2)\sin\varphi_2-4\omega\zeta_2 C\cos\varphi_2=0$$

$$-\alpha A^2 B\omega^2\cos 2\varphi_1+C(1-4\omega^2-\frac{\alpha}{2}A^2\omega^2)\cos\varphi_2+4\omega\zeta_2 C\cos\varphi_2=F_0$$

From the first two equations, A=0 is a solution, then B=0 from the third equation, representing the pure bending response written as

$$y(t)=C\cos(2\omega t-\varphi_2)$$

$$C=\frac{F_0}{\sqrt{(1-4\omega^2)^2+(2\omega\zeta_2)^2}},$$

$$\varphi_2=\tan^{-1}\frac{2\omega\zeta_2}{1-4\omega^2}$$

When $A\neq0$, the solution is associated with

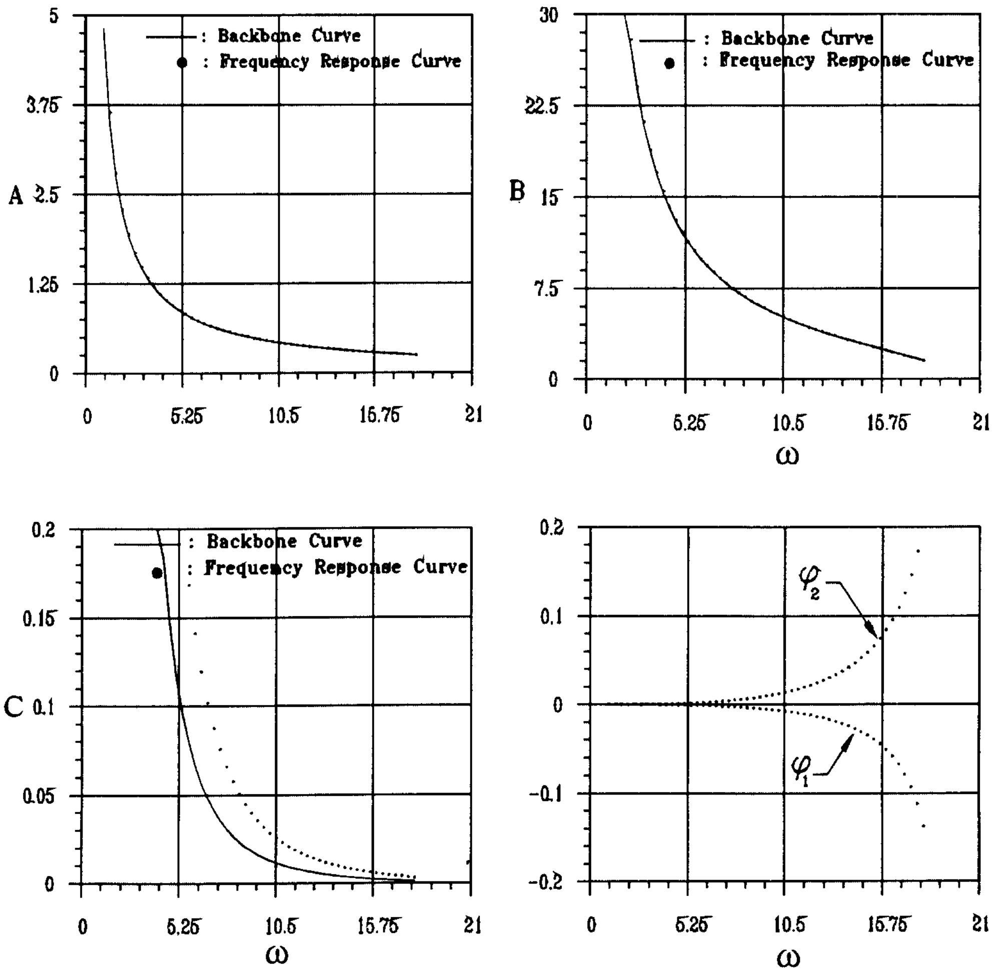

Fig. 13 Frequency response curves associated with nonlocal mode in damped and forced system ($\alpha=0.1$, p=20, $F_0=1.0$, $\zeta_1=\zeta_2=10^{-4}$)

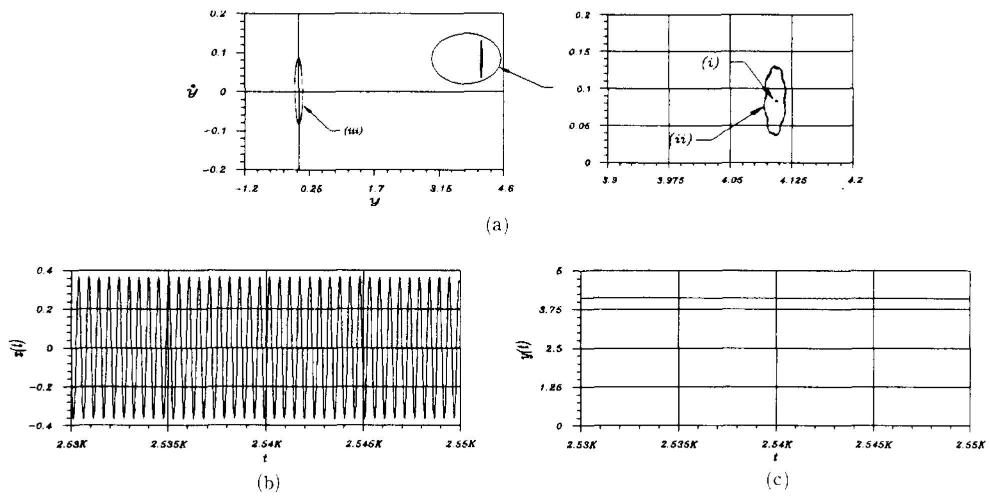

Fig. 14 A numerically computed responses of Eq. (20) (a) Poincaré map in the y-y plane. Three initial conditions are used to show stability of the nonlocal mode response. Point (i) corresponds to the exact nonlocal mode response, Point (ii) to the near nonlocal mode response and Point (iii) to the bending mode response. Points (ii) and (iii) are attracted to their respective attractor, but approach very slowly due to small damping. (b), (c) Time histories of x (t) and y (t) for the nonlocal mode response ($\alpha=0.1$, $p=20$, $\omega=12.2$, $F_0=1.0$, $\zeta_1=\zeta_2=10^{-4}$)

nonlocal mode and solved by using MATLAB[1] as shown in Fig. 13 and in order to verify the periodicity and stability of responses Poincaré map and time responses are computed and shown in Fig. 14. The response is shown in Fig. 14 to be periodic and asymptotically stable. It has been found by Lee (1995) that the forced response is periodic in the excitation frequency range narrower than that of nonlocal mode when damping are present. For small damping and forcing amplitudes, it is possible to obtain two attracting periodic motions; one is the pure bending response, and the other one associated with nonlocal mode. The domain of attraction determines the set of initial conditions for each attractor.

7. Conclusion

The dynamic lateral instability of a thin beam has been demonstrated by showing the existence of periodic torsional vibrations having finite amplitudes under small periodic bending loads. If the periodicity of forced responses is not necessarily required for the lateral instability, then much broad set of systems parameters will result in the lateral instability. The basic theory, described in this study to compute bifurcation mode and the associated forced responses, may be applicable to other systems.

1) A software package for scientific and engineering numeric computation by *The Mathworks, Inc.*

Acknowledgement

The author wishes his gratitude to Inha University for the financial support to this study.

References

Birkhoff, G. D., 1927, *Dynamical Systems*, A. M. S. Publication.

Bolotin, V. V., 1964, *The Dynamic Stability of Elastic Systems*, Holden Day.

Crespo da Silva, M. R. M. and Glynn, C. C., 1978A, "Nonlinear Flexural-Flexural -Torsional Dynamics of Inextensional Beams, Part I. Equations of motion," 6 (4), *J. Structural Mechanics*, pp. 437～448.

Crespo da Silva, M. R. M. and Glynn. C. C., 1978B, "Nonlinear Flexural-Flexural-Torsional Dynamics of Inextensional Beams, Part II. Forced Motions," 6 (4) *J. Structural Mechanics*, pp. 449 ~461.

Cusumano, J. P. and Moon, F. C., 1995A, "Chaotic Non-Planar Vibrations of the Thin Elastica, Part I. Experimental Observation of Planar Instability," *J. Sound and Vibration*, 179 (2), pp. 185~208.

Cusumano, J. P. and Moon, F. C., 1995B, "Chaotic Non-Planar Vibrations of the Thin Elastica, Part II. Derivation and Analysis of a Low-dimensional Model," *J. Sound and Vibration*, 179 (2), pp. 209~226.

E. Ott, 1993, *Chaos in Dynamical Systems*, Cambridge Univ. Press.

Guckenheimer, J. and Holmes, P. J., 1983, *Nonlinear Oscillations, Dynamical Systems and Bifurcations of Vector Fields*, Springer — Verlag, N. Y.

Harvey, T. and Alto, P., 1958, "Natural Forcing Functions in Nonlinear Systems," *J. Appl. Mech.*, pp. 352~356.

Johnson, T. and Rand, R. H., 1979, " On the Existence and Bifurcation of Minimal Normal Modes," *Int. J. of Nonlinear Mechanics*, Vol. 10 4, pp. 1~12.

Kim, M. K., 1995, "Experiments on Nonlinear Vibrations of Cantilevered Beam," *M. S. Thesis*, Inha University.

Lee, Y. S., 1995, "On the Chaotic Vibrations of Thin Beams by a Bifurcation Mode," *MS Thesis*, Inha Univ.

Magnus, W. and Winkler, S., 1966, *Hill's Equation*, Interscience.

McLachlan, N. W., 1964, *Theory and Application of Mathieu Functions*, Dover Publications, N. Y.

Meirovitch, L., 1970, *Methods of Analytical Dynamics*, McGraw-Hill, N. Y.

Nayfeh, A. H. and Mook, D. T., 1979, *Nonlinear Oscillations*, New York, Wiley-Interscience.

Nayfeh, A. H. and Pai, P. F., 1989, "Nonlinear Nonplanar Parametric Responses of an Inextensional Beam," *Int. J. Nonlinear Mechanics*, Vol. 24, No. 2, pp. 139~158.

Pai, P. and Nayfeh, A. H., 1990, "Nonlinear Nonplanar Oscillations of a Cantilever Beam under Lateral Base Excitations," *Int. J. Non-Linear Mech.*, 25 (5), pp. 455~474.

Pak, C. H., 1988, " On the Stability Behaviors of Bifurcated Normal Modes in Coupled Nonlinear Systems," *J. Applied Mechanics,* Vol 56, pp. 155~161.

Pak, C. H., and Rosenberg, R. H., 1968, "On the Existence of Normal Modes Vibrations in Nonlinear Systems," *Q. Appl. Math.*, Vol 24, pp. 177~193.

Pak, C. H., Rand, R. H. and Moon, F. C., 1992, "Free Vibrations of a Thin Elastica," *Nonlinear Dynamics*, 3, pp. 347~364.

Rand, R. H., Pak, C. H. and Vakakis, A. F., 1992, " Bifurcation of Nonlinear Normal Modes in a Class of Two Degree of Freedom System", *Acta Mechanica*, Vol. 3, pp. 129~145.

Rosenberg, R. M., 1966, "On Nonlinear Vibrations of Systems with Many Degrees of Freedom," *Advances in Applied Mechanics* 9, pp. 155~242, Academic Press.

Synge, J. L., 1962, "On the Geometry of Dynamic," Vol. 226, pp. 31~106.

Timoshenko, S., 1934, *Theory of Elastic Stability*, McGraw-Hill.

Vakakis, A. F., 1991, " Analysis and Identification of Linear and Nonlinear Normal Modes in Vibrating Systems," *PhD Thesis*, Caltech.